

# Quantification of $pn$ -Junction Recombination in Interdigitated Back-Contact Crystalline Silicon Solar Cells

Pierpaolo Spinelli, Bas W. H. van de Loo, Ard H. G. Vlooswijk, W. M. M. Kessels, and Ilkay Cesar

**Abstract**—Interdigitated back-contact (IBC) solar cells based on diffused crystalline silicon comprise a series of  $pn$ -junctions which border at the rear surface of the wafer. In this work, it is established that the presence of these  $pn$ -junctions can induce significant additional charge-carrier recombination, which affect the conversion efficiency of IBC cells through a reduction in fill factor and open-circuit voltage. Using specialized test structures with varying length of  $pn$ -junctions per area of solar cell (i.e., with varying junction density), the magnitude of the recombination at the  $pn$ -junction was determined. For nonpassivated rear surfaces, a second-diode recombination current density per unit of junction density  $J_{02}$  of  $\sim 61 \text{ nA} \cdot \text{junction}^{-1} \cdot \text{cm}^{-1}$  was measured, whereas for surfaces which were passivated by either  $\text{SiN}_x$  or  $\text{Al}_2\text{O}_3/\text{SiN}_x$ ,  $J_{02}$  was reduced to  $\sim 0.4 \text{ nA} \cdot \text{junction}^{-1} \cdot \text{cm}^{-1}$ . Therefore, passivation of defects at the rear surface was proven to be vital in reducing this characteristic recombination current. Finally, by optimizing the  $p$ - and  $n$ -type dopant diffusion process recipes,  $J_{02}$  recombination could be suppressed. The improved doping recipes led to an increase in conversion efficiency of industrial “mercury” IBC solar cells by  $\sim 1\%$  absolute.

**Index Terms**—Depletion region recombination, interdigitated back contact (IBC),  $pn$ -junction, surface passivation, solar cells.

## I. INTRODUCTION

IN INTERDIGITATED back-contact (IBC) solar cells, both the positive and negative contacts are located at the rear side, to avoid parasitic shading losses by front side metallization. Despite this advantage, the performance of IBC solar cells can be significantly reduced by a lower short-circuit current density ( $J_{sc}$ ), for instance due to lateral transport losses of charge carriers toward the rear contacts, an effect known as “electrical shading” [1]. To reduce such losses, crystalline silicon (c-Si) solar cells with a diffused “front floating emitter” (FFE) have

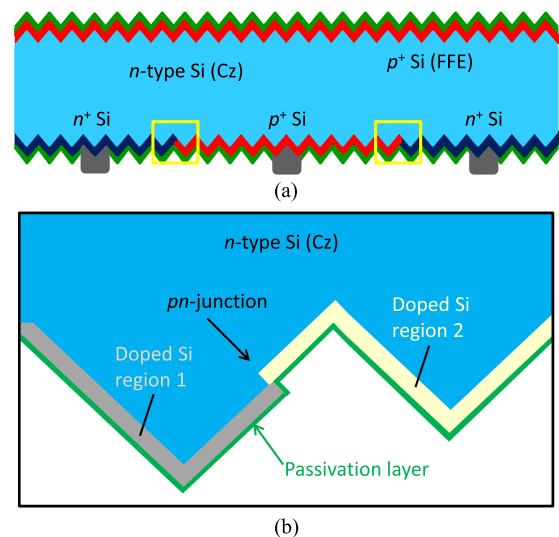


Fig. 1. (a) Schematic of the ECN IBC cell Mercury, which comprises a front-floating emitter. (b) A close-up of the rear-side  $pn$ -junction.

been developed (see Fig. 1), in which the lateral conduction of minority carriers takes place via a highly doped region near the front surface [2], [3]. In this way, high  $J_{sc}$  values can be achieved with minimal constraints to rear side patterning. ECN’s IBC concept Mercury, based on an FFE, has so far reached conversion efficiencies up to 21.1% [4], [5]. Although the problems of electrical shading thus can be minimized, in this work it will be shown that another mechanism can induce a significant loss in performance for diffused-junction IBC solar cells. Specifically, it will be shown that a distinctive charge-carrier recombination current can be associated with the presence of the  $pn$ -junctions which border at the rear surface of the solar cell.

In semiconductor physics, it is known that additional charge-carrier recombination can occur when a  $pn$ -junction borders a surface [6], [7]. First of all, it follows from the Shockley–Read–Hall theory that defect states within the band gap are most effective when electrons and holes are captured with equal rates. This is when the condition

$$n \cdot \sigma_n = p \cdot \sigma_p \quad (1)$$

is satisfied, with  $n$  and  $p$  being the electron and hole carrier densities, and  $\sigma_n$  and  $\sigma_p$  the electron and hole capture cross sections

Manuscript received December 16, 2016; revised February 22, 2017, April 20, 2017, and May 19, 2017; accepted May 29, 2017. Date of publication June 29, 2017; date of current version August 18, 2017. This work was supported by the Dutch Ministry of Economic Affairs, via the Top Sector Alliance for Knowledge and Innovation program IBChampion. P. Spinelli and B. W. H. van de Loo contributed equally to this work. (Corresponding author: Bas W. H. van de Loo.)

P. Spinelli and I. Cesar are with ECN Solar Energy, Petten 1755 ZG, The Netherlands (e-mail: spinelli@ecn.nl; cesar@ecn.nl).

B. W. H. van de Loo and W. M. M. Kessels are with the Eindhoven University of Technology, Eindhoven 5600 MB, The Netherlands (e-mail: b.w.h.v.d.loo@tue.nl; w.m.m.kessels@tue.nl).

A. H. G. Vlooswijk is with Tempres Systems BV, Vaassen 8171 MD, The Netherlands (e-mail: avlooswijk@tempres.nl).

Color versions of one or more of the figures in this paper are available online at <http://ieeexplore.ieee.org>.

Digital Object Identifier 10.1109/JPHOTOV.2017.2714134

of the defects, respectively [8], [9]. Under such conditions, the recombination current  $J_{\text{rec}}$  is given by

$$J_{\text{rec}} = J_{02} \cdot \exp(V/mV)$$

with  $m$  being the ideality factor (in this case  $m = 2$ ),  $V$  the voltage,  $V_t$  the thermal voltage, and  $J_{02}$  the second-diode recombination parameter. As the electron and hole densities change sharply across the  $pn$ -junction, condition (1) is typically satisfied somewhere across the junction, such as in its depletion region [10], [11]. The so-called “depletion region recombination” which occurs as a result, is particularly pronounced where the  $pn$ -junction borders a surface, as at a surface often a high density of defect states is present. In fact, any depleted surface near the bordering  $pn$ -junction can lead to severe  $J_{02}$ -type recombination, due to efficient transport of charge-carriers through the highly doped  $p$ - and  $n$ -type regions toward this recombination active region [12]. **The recombination at the depleted surface near the  $pn$ -junction can be about one order of magnitude higher than the recombination in the depletion region of the junction** [12].

Second, adjacent highly doped  $n$ - and  $p$ -type Si regions can induce a tunneling recombination current between the conduction band of  $n^+$  Si and the valence band of  $p^+$  Si. Such tunneling recombination current occurs in particular for abrupt, highly doped  $pn$ -junctions and is aided by defect states that are present within the band gap (such as at the c-Si surface) which facilitate trap-assisted tunneling [13].

**Although the above-mentioned recombination mechanisms have a different physical nature, in practice it can be hard to discern amongst** them. Therefore, we will simply refer to them together as “ $pn$ -junction recombination” pathways.

Also for c-Si solar cells in specific, signs of a significant  $J_{02}$ -recombination path for charge carriers have been observed when a  $pn$ -junction terminates at a surface (or at the perimeter of the cell) that is poorly or not passivated [14]–[17]. For monocrystalline front-contacted solar cells, surface bordering of the  $pn$ -junction occurs only at the edge of the wafer. Hence, its detrimental effects on the performance of the solar cells, such as a reduced fill factor  $FF$  and reduced  $V_{\text{oc}}$  at low light intensities, are in general minimal. In IBC cells, however, the length of  $pn$ -junction which borders at the surface is significantly larger per unit area. Therefore, the question arises whether for IBC solar cells the above-mentioned  $J_{02}$ -type recombination channels might still induce a significant loss mechanism.

Recent publications provide indications that  **$pn$ -junction recombination can indeed significantly affect the conversion efficiency of IBC solar cells**. For instance, Müller *et al.* [3] found a reduction in efficiency of diffused-junction IBC cells by 2% absolute after placing the cell under reverse bias. The reduction in efficiency was in part attributed to an increase in  $J_{02}$  from 12 to 82 nA/cm<sup>2</sup>. A plausible explanation for the increase in  $J_{02}$  was the degradation of the rear surface passivation layer, which would affect the recombination at the bordering  $pn$ -junction. Yet, the presence of this recombination mechanism could not be verified.

Additionally, Dong *et al.* [18] found by simulating the tunneling recombination current between the  $n^+$  and  $p^+$  Si in IBC

solar cells that tunneling can be significant for solar cells under forward bias, and that the profile of boron dopants had a pronounced influence on the tunneling recombination.

Peibst *et al.* found that an additional  $pn$ -junction recombination current was required to fit Suns- $V_{\text{oc}}$  characteristics of high-efficiency homojunction IBC solar cells where the  $n^+$  and  $p^+$  Si regions were passivated independently [19], whereas such recombination current was not found for passivation of the rear-surface by  $\text{Al}_2\text{O}_3/\text{SiN}_x$  or thermal  $\text{SiO}_2$  [19], [20]. Nevertheless, in all cases, the choice of the rear-surface passivation scheme had a large influence on the obtained pseudo-fill factor ( $pFF$ ) [19], [20].

Finally, indications for a recombination channel at or near the  $pn$ -junction have also been found for IBC solar cell concepts which are not based on diffused junctions, but which comprise  $n^+$  and  $p^+$ -type doped polycrystalline Si (poly-Si) passivating contacts. For instance, for lifetime samples with interdigitated  $p$ - and  $n$ -type doped poly-Si contacts, minority carrier lifetime data could only be fitted using a diode with local ideality factor  $n > 1$ , whereas for samples without rear interdigitated junctions such nonideal recombination current was absent [21]. Interestingly, by creating a gap between the  $n^+$  and  $p^+$  poly-Si regions, the open-circuit voltage  $V_{\text{oc}}$  as well as the  $pFF$  of the IBC solar cell increased significantly [22]. Nonetheless, the creation of a gap between the  $p$  and  $n$ -type poly-Si regions imposes additional and complex process steps (as it also does for IBC solar cells based on diffused c-Si junctions) and is, therefore, undesirable from an industrial point of view.

Despite the potential detrimental effects of  $pn$ -junction recombination on IBC solar cells, a systematic study or quantification of this recombination mechanism is still lacking. Therefore, in this work, the charge-carrier recombination at the  $pn$ -junction was systematically investigated by using dedicated test structures, in which the density of  $pn$ -junctions (or the pitch of the  $pn$ -junctions) was varied. The recombination at the  $pn$ -junction was examined for unpassivated rear surfaces, as well as for surfaces which were passivated by industrially relevant passivation schemes, i.e., nitric acid oxidation of Si (NAOS) in combination with a  $\text{SiN}_x$  or an  $\text{Al}_2\text{O}_3/\text{SiN}_x$  stack as capping layer. Finally, the influence of the boron and phosphorus diffusion process recipe on recombination at the  $pn$ -junction was studied on test structures as well as on completed IBC solar cells. It will be shown that by careful tuning of the diffusion recipe, the conversion efficiency of IBC *Mercury* cells could be improved by  $\sim 1\%$  absolute, which relates to a reduction of  $pn$ -junction recombination.

## II. EXPERIMENTAL

To assess recombination at the  $pn$ -junction, specialized test wafers were made. Fig. 2 shows a schematic of the test structures (a) and a photograph of a test wafer (b). The test wafers were fabricated by the same process steps as used for the mercury solar cells (see Fig. 1) [2], with the exception of the patterning design of the  $p$ - and  $n$ -type doped regions at the rear surface. As a base material, **6-in, Czochralski-grown,  $n$ -type Si wafers with a resistivity of  $\sim 5 \Omega\cdot\text{cm}$**  were used.

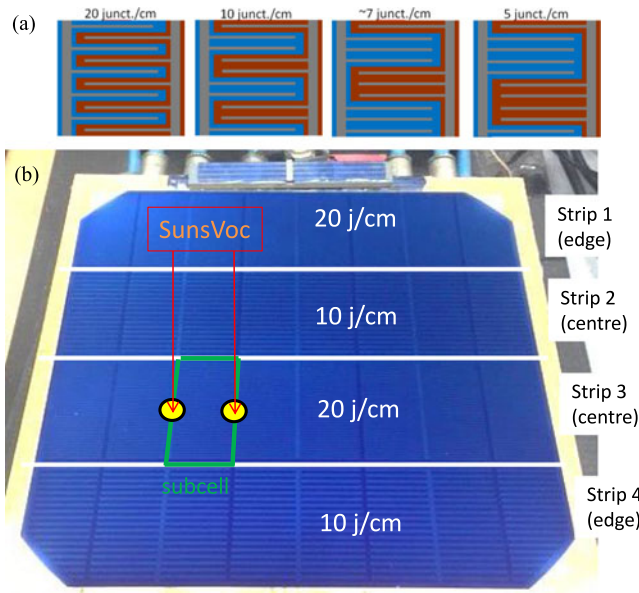


Fig. 2. (a) Schematic of the subcells present in the test wafers which were used to monitor  $pn$ -junction recombination. The subcells have a varying  $pn$ -junction density, ranging from 5 to 30 junctions/cm. The red and blue lines represent the  $p^+$  and  $n^+$  Si regions, respectively, whereas the grey areas represent the metal contacts, which are applied by screen printing and a high-temperature “firing” step. (b) Photograph of a 6” test wafer comprising four rows of eight subcells, which contain eight identical subcells of  $1.9 \times 3.8 \text{ cm}^2$ , with in this case 10 or 20 junctions/cm. The typical positions where the electrodes of the Suns- $V_{oc}$  set-up contact the subcell are indicated. For the purpose of this photograph, the highly doped regions were not contacted by metal.

After random pyramid texturing by alkaline (KOH) etching, boron and phosphorus diffusions were carried out in a horizontal tube furnace (Tempress Systems) to form the heavily doped  $p$ - and  $n$ -type regions, respectively. The interdigitated pattern at the rear surface was obtained using a screen-printed resist in combination with subsequent wet-chemical removal of the highly doped Si, before carrying out the next diffusion step. **In this work, three different boron and phosphorus (co-)diffusion recipes were studied (they were not independently varied), labeled A, B, and C.** Fig. 3 shows the doping concentration profiles as determined by electrochemical capacitance–voltage measurements. Afterwards, the wafer was subjected to a short wet etch to create the desired doping profiles. After the diffusion steps, the phosphorus- and boron-containing glass was removed. Subsequently, the front and rear Si surfaces were oxidized simultaneously using a nitric acid dip at room temperature (NAOS). Next,  $\text{Al}_2\text{O}_3$  was deposited on the front surface using spatial atomic layer deposition (Levitrack, Levitech), after which it was capped by plasma-enhanced chemical vapor deposited  $\text{SiN}_x$ . The rear surface (where the  $pn$ -junctions border) was either passivated by capping the thin oxide, (formed by NAOS), either by a single layer of  $\text{SiN}_x$ , a stack of  $\text{Al}_2\text{O}_3/\text{SiN}_x$ , or no capping at all (termed “no passivation”). Note that the passivation performance of the  $\text{SiN}_x$  significantly changes by the used nitric-acid oxidation of the Si [23]. Finally, the passivated and doped Si regions at the rear were contacted by screen-printed Ag paste followed by a high-temperature “firing” step.

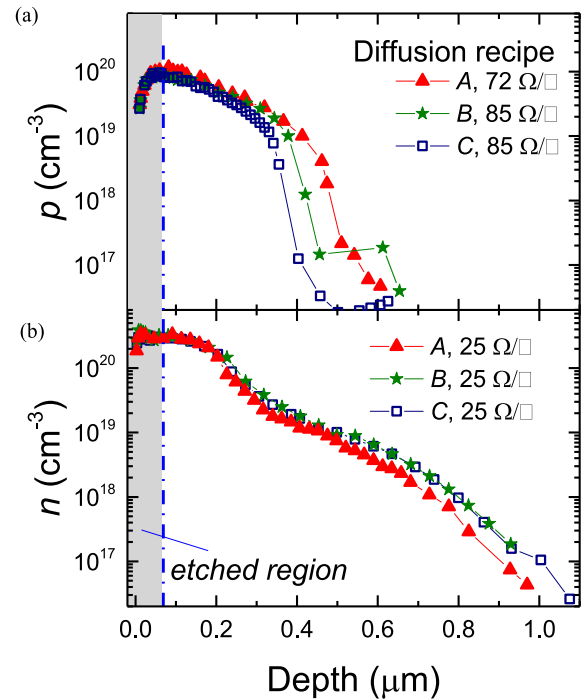


Fig. 3. Electrochemical capacitance-voltage (ECV) measurements of the dopant profiles of (a) the boron- and (b) the phosphorus-doped regions for the three different (co-)diffusion recipes A, B, and C. The first 60 nm was etched back to obtain the desired doping profiles. The sheet resistance was determined by four-point probe measurements for each doped region after etch-back.

At the front surfaces of the test structures as well as of the IBC Mercury solar cells, a homogeneously doped  $p^+$  Si FFE was present. At the rear surface of the test structures, the length of the  $pn$ -junction was varied by changing the “linear”  $pn$ -junction density from 5 to 20 junctions per centimeter [see Fig. 2(a)]. Specifically, the equal widths of both the  $n^+$  and  $p^+$  Si regions on the test structures were varied from 500 to 1000, 1500, and 2000  $\mu\text{m}$ , whereas the total area of  $n^+$  Si or  $p^+$  Si was identical for each test structure. In contrast, in actual IBC Mercury cells, a typical junction density of  $15 \text{ cm}^{-1}$  is used with unequal widths of the  $n^+$  and  $p^+$  Si region. The metal contact area was kept equal between all test structures as well, and was similar to the metal coverage used in IBC Mercury solar cells.

After metallization, each subcell was measured in a Suns- $V_{oc}$  setup (Sinton Instruments) by contacting the adjacent positive and negative busbars by electrodes. Note that only the test structures in the center of the wafer were used to prevent “edge effects,” which showed a significant higher recombination [5], [27]. It was verified by laser cutting of the individual subcells that there was no cross correlation between them. **By fitting the Suns- $V_{oc}$  measurements to a two-diode model,  $J_{01}$ ,  $J_{02}$ ,  $pFF$ , and shunt resistance  $R_{Shunt}$  were extracted. In all cases, the  $R_{Shunt}$  values were found to be too high to be reliably extracted, and only a lower limit could be derived.** Even though Suns- $V_{oc}$  measurements provide only data from  $\sim 0.5 \text{ V}$  onwards, (see e.g., Fig. 4), the values of  $J_{01}$ ,  $J_{02}$  had a unique influence on the Suns- $V_{oc}$  fit and could, therefore, be reliably extracted. Nevertheless, considerable difference in  $J_{01}$  and  $J_{02}$  has been found when cross-checking the obtained values with



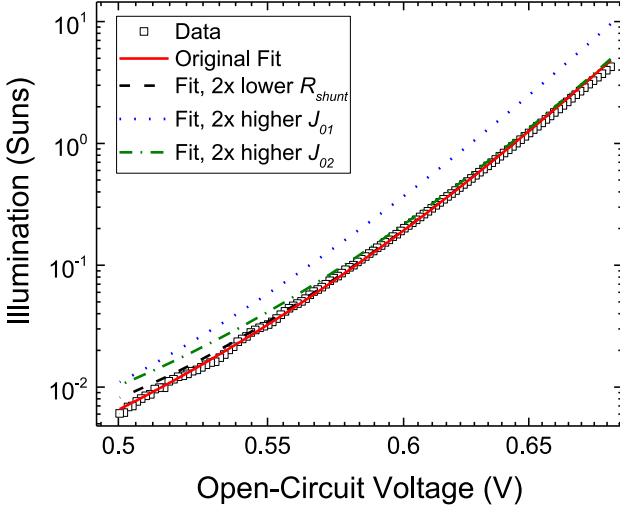


Fig. 4. Example of Suns- $V_{oc}$  data and the fit by a two-diode model of a test structure comprising 20 junctions/cm<sup>2</sup> (doping recipe C, Al<sub>2</sub>O<sub>3</sub>/SiN<sub>x</sub> passivation). The dashed lines indicate the changes induced by manipulation of one of the fit parameters of the two-diode model.

dark  $I$ - $V$  and light  $I$ - $V$  measurements. In other work, different results between these measurements techniques have also been reported [17], and care must, therefore, be taken when comparing  $J_{01}$  and  $J_{02}$  parameters derived by Suns- $V_{oc}$  with values derived by dark  $I$ - $V$  and light  $I$ - $V$ . In the remaining of this work, all  $J_{01}$  and  $J_{02}$  values are derived from Suns- $V_{oc}$  measurements.

### III. RESULTS

#### A. Influence of Surface Passivation on $pn$ -Junction Recombination

First, the test structures with unpassivated rear surface were examined. The structures were prepared using diffusion recipe B. The homogeneously doped  $p^+$  Si front surfaces (the “FFE”) were passivated by a stack of Al<sub>2</sub>O<sub>3</sub>/SiN<sub>x</sub>. For this specific experiment without rear-surface passivation, no screen-printed metal contacts were applied to prevent shunting, although a firing step was carried out. Therefore, in this case the electrodes of the Suns- $V_{oc}$  setup were put in direct contact with the  $n^+$  and  $p^+$  Si regions. The results of the Suns- $V_{oc}$  data, fitted to a two-diode model, are shown in Fig. 5(a)–(c).

As can be seen in Fig. 5(a),  $J_{01}$  is approximately constant with the junction density, and has a relatively high value of  $2540 \pm 400$  fA/cm<sup>2</sup>, which is typical for doped surfaces that are not passivated. In contrast,  $J_{02}$  shows a linear increase with the junction density at a rate of  $61 \pm 5$  nA·junction<sup>-1</sup>·cm<sup>-1</sup> and thus reveals  $pn$ -junction recombination [see Fig. 5(b)]. Moreover, the  $pFF$  [see Fig. 5(c)] and  $V_{oc}$  at 1-sun illumination (not shown) decrease significantly with the density of junctions, the latter from 583 mV at a junction density of 5 cm<sup>-1</sup> to 553 mV at a density 20 cm<sup>-1</sup>.

For comparison, also the  $FFJ_{01}$ , which is the fill-factor in case it is only limited by  $J_{01}$ -type recombination, is shown in Fig. 5(c).  $FFJ_{01}$  was evaluated from  $V_{oc}$  at 1-sun using the exact analytical solution of [24]. The difference be-

tween  $FFJ_{01}$  and the  $pFF$  for a two diode model in principle can only be attributed to losses due to the parasitic shunting, ( $\Delta FF_{R_{sh}}$ ), or  $J_{02}$ -type recombination, ( $\Delta FF_{J_{02}}$ ):  $pFF = FFJ_{01} - \Delta FF_{R_{sh}} - \Delta FF_{J_{02}}$ .

The shunt resistance  $R_{shunt}$  for all test structures was too high to be determined via the Suns- $V_{oc}$  measurements. Considering the strong increase in  $J_{02}$  with the junction density, it is most likely that the observed decrease in  $pFF$  with increasing junction density, therefore, predominantly originates from  $J_{02}$ -type recombination.

In the case of a passivated rear-surface [see Fig. 5(d)–(f)],  $J_{01}$  is significantly reduced compared to the unpassivated case, with lower  $J_{01}$  values for Al<sub>2</sub>O<sub>3</sub>/SiN<sub>x</sub> than for SiN<sub>x</sub> passivation. For both passivation schemes,  $J_{01}$  is independent of the junction density. Also, the  $J_{02}$  values are significantly reduced when the surface is passivated for all junction densities, with higher  $J_{02}$  values for Al<sub>2</sub>O<sub>3</sub>/SiN<sub>x</sub> than for SiN<sub>x</sub>. Despite the significantly reduced  $J_{02}$  values after passivation, an increase in  $J_{02}$  with junction density of  $\sim 0.4$  nA·junction<sup>-1</sup>·cm<sup>-1</sup> for Al<sub>2</sub>O<sub>3</sub>/SiN<sub>x</sub> and SiN<sub>x</sub> can still be observed. Note that  $J_{02}$  for the passivated case is extrapolated to 0 junctions/cm, still a  $J_{02}$  current of 6–8 nA/cm<sup>2</sup> is found, which is related to recombination in other parts of the cell.

The  $pFF$  for the case that the test structures are passivated decreases with increasing junction density, albeit to a much lesser extent than in the case of an unpassivated rear surface. Also, when the rear surface is passivated, the shunt resistance values are too high to be determined by fitting a two-diode model to the Suns- $V_{oc}$  data. The decrease in  $pFF$  with junction density (and the highest  $pFF$  values for SiN<sub>x</sub>) can qualitatively be explained well by the trends in  $J_{02}$  with junction density, where high  $J_{02}$  values reduce the  $pFF$ .

Despite the significantly lower  $J_{02}$  recombination per density of junction for the passivated surface compared to the unpassed surface, for the passivated surfaces still a  $J_{02}$ -type recombination pathway can be associated with the density of  $pn$ -junctions which is reducing the  $pFF$  and  $V_{oc}$  of the test structures. In the next paragraph, we will further reduce this pathway by adjusting the dopant profiles.

#### B. Influence of the Diffusion Recipe on $pn$ -Junction Recombination

Next, the influence of the diffusion recipe on  $pn$ -junction recombination was evaluated. To this end, the Suns- $V_{oc}$  data obtained from test structures with three different diffusion recipes were again fitted by the two-diode model. The rear surfaces of the test structures (where the  $pn$ -junctions border) were passivated by Al<sub>2</sub>O<sub>3</sub>/SiN<sub>x</sub>, which yielded the lowest  $J_{01}$  values in the previous section.

As can be seen in Fig. 6, diffusion recipe A shows a clear increase in  $J_{02}$  recombination with increasing junction density at a rate of  $\sim 1.6$  nA·junction<sup>-1</sup>·cm<sup>-1</sup>. Note that this increase in  $J_{02}$  is even more significant for diffusion recipe A than for recipe B, which was used in the previous section. Remarkably, for diffusion recipe A, even the  $J_{01}$ -type recombination increases with  $\sim 20$  fA·junction<sup>-1</sup>·cm<sup>-1</sup>. As a result of the increase in  $J_{01}$  and

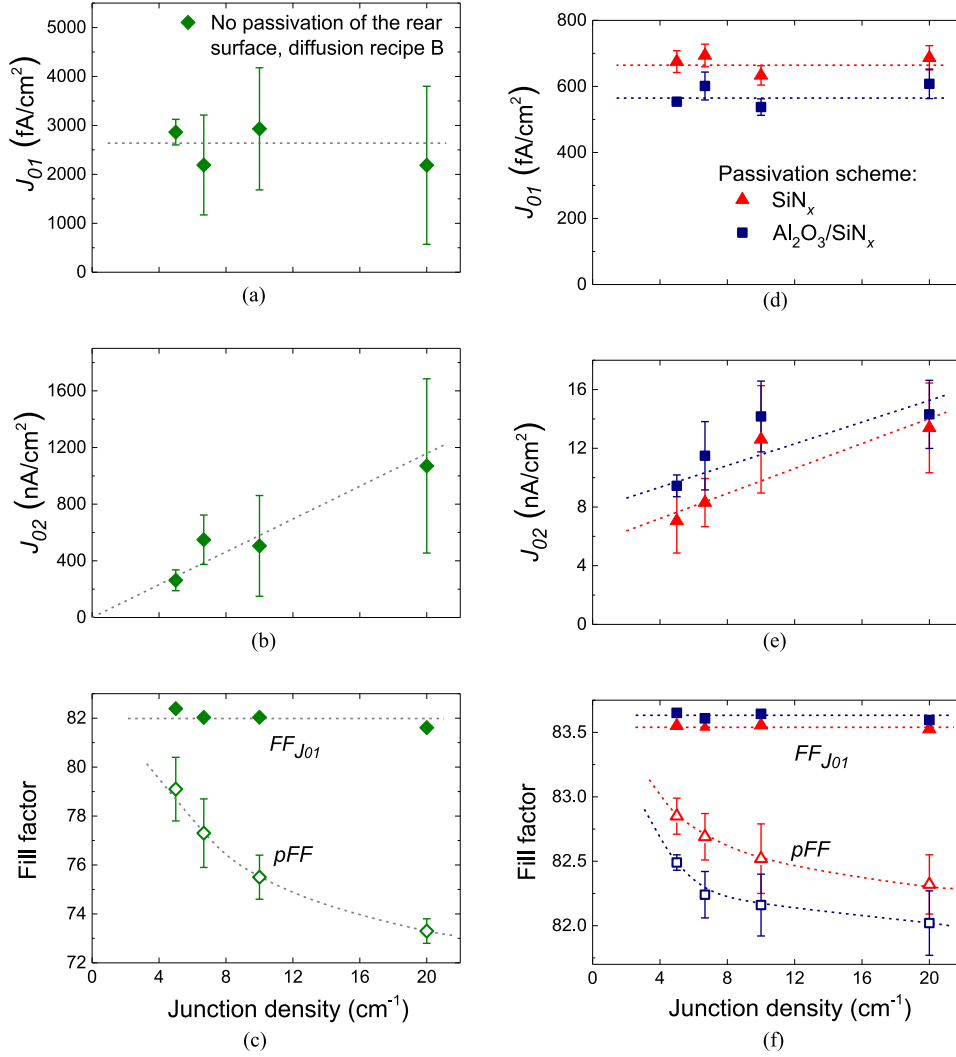


Fig. 5. Results from fitting Suns- $V_{oc}$  measurements to a two-diode model, for test structures prepared by diffusion recipe B for (a)–(c) samples without rear-surface passivation and (d)–(f) samples where the rear surface is passivated by either  $\text{Al}_2\text{O}_3/\text{SiN}_x$  or  $\text{SiN}_x$ . The upper limit of the fill factor  $FF_{J01}$  shown in (c) and (f) is derived from the open-circuit voltage at one sun using the (exact) analytical method described in [24]. Lines are guides for the eye.

$J_{02}$ , a decrease in  $V_{oc}$  of about 10 mV is observed when the junction density is increased from 5 to 20  $\text{junction}^{-1}\cdot\text{cm}^{-1}$  [25]. Moreover, the results show a very strong decrease in  $pFF$  with increasing junction density. Interestingly, for recipe C virtually no additional  $J_{01}$  and  $J_{02}$  recombination is observed with increasing junction densities, nor is a decrease in  $pFF$  observed. Therefore, this experiment demonstrates that by tuning the diffusion recipe any significant  $pn$ -junction recombination can practically be avoided, even in case of a gap-less  $pn$ -junction. The latter is particularly important for a cost-effective processing of IBC solar cells.

Next, the influence of the different diffusion recipes on IBC solar cells was studied. To this end, full-area (6-in) IBC Mercury solar cells were fabricated using diffusion recipe C and recipe A. The solar cell parameters for both groups were evaluated from light  $J-V$  and suns- $V_{oc}$  measurements as shown in Table I. Note that the cell efficiencies obtained here are about  $\sim 1.8\%$  absolute lower than the current record efficiencies for Mercury cells of

21.1% [5]. Nonetheless, both groups of solar cells are, apart from the diffusion step, fabricated in the same process run and, therefore, allow for a close comparison to discriminate the effect of the diffusion step on the solar cell performance.

The largest relative improvements for recipe C compared to recipe A are the reduction in  $J_{01}$  and  $J_{02}$  by  $\sim 40\text{--}50\%$ . As a result, the efficiency of the IBC cells improves by 1% absolute from 18.3% to 19.3%. The  $J_{01}$  and  $J_{02}$  values obtained for finalized solar cells are approximately in line with the results on test structures, despite the fact that the finalized IBC cells also incorporate the edges of the wafer, which in our previous work showed a notable higher  $J_{01}$  recombination current [5].

#### IV. DISCUSSION

In Section III-A, it was shown that the  $J_{02}$  recombination, which is associated with the density of  $pn$ -junctions, can be reduced considerably from  $\sim 61 \text{ nA}\cdot\text{junction}^{-1}\cdot\text{cm}^{-1}$  (without

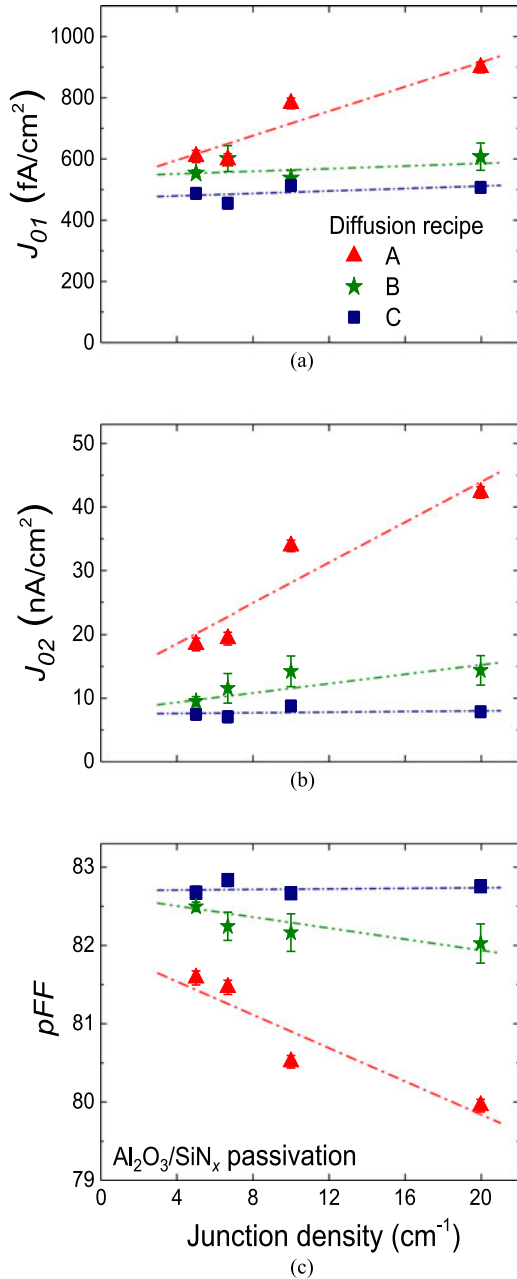


Fig. 6.  $J_{01}$ ,  $J_{02}$ , and  $pFF$  are extracted from Suns- $V_{oc}$  measurements on test structures, which are prepared using three different diffusion recipes. A stack of  $\text{Al}_2\text{O}_3/\text{SiN}_x$  was used for the passivation of the rear-side, where the  $pn$ -junctions were present. Lines are linear fits to the data.

surface passivation) to values below  $<1.6 \text{ nA} \cdot \text{junction}^{-1} \cdot \text{cm}^{-1}$  (after surface passivation). Surface passivation is, therefore, of key importance in the reduction of  $J_{02}$  recombination in IBC solar cells. This importance of surface passivation can (as was discussed in Section I) for a part be attributed to a very efficient charge transport of minority carriers to the surface near the  $pn$ -junction. As a consequence of this transport, surface recombination will not become limited by the diffusion of minority charge carriers. Note that this also holds for IBC cells which comprise a gap between the  $p$ - and  $n$ -type highly doped regions, as has also been found by simulations of IBC cells

[26]. Furthermore, efficient carrier transport can also take place through the space-charge region induced by the fixed charge in the passivation scheme, as has been observed in, e.g., Ref. [27].

Even though passivation of the rear surface of IBC solar cells is thus of high importance, the passivation of interdigitated  $n^+$  and  $p^+$  Si surfaces can especially near the  $pn$ -junction be challenging. For instance, as the net doping level along the surface where the  $pn$ -junction borders changes from  $n$ - to  $p$ -type, the fixed charge density of the passivation scheme will at some point not provide field-effect passivation any more. For example, for surface passivation by  $\text{Al}_2\text{O}_3$ , it is experimentally and theoretically demonstrated that the negative fixed charge (of typically  $-5 \cdot 10^{12} \text{ cm}^{-2}$ ) does not provide field-effect passivation for  $n^+$  Si surfaces having a (net) local  $n$ -type doping concentration around  $\sim 10^{19} \text{ cm}^{-3}$  [28], [29]. Therefore, in particular excellent *chemical* passivation of the rear surface of IBC cells is preferred to avoid surface recombination at these regions near the  $pn$ -junction. In this work, it was found that significant  $pn$ -recombination could be avoided when using the  $\text{Al}_2\text{O}_3/\text{SiN}_x$  passivation scheme.

Apart from the surface passivation scheme, the presence and magnitude of  $pn$ -junction recombination were also found to be dependent on the diffusion recipe employed. For the surfaces passivated by  $\text{Al}_2\text{O}_3/\text{SiN}_x$ , the highest  $J_{02}$ -recombination current per junction was observed for the diffusion recipe that also resulted in the highest  $J_{01}$  values, not only on test structures (see Fig. 6) and finalized solar cells (see Table I), but also on uniformly doped surfaces (not shown). As the diffusion profiles of all recipes are similar (see Fig. 3), the differences in  $J_{01}$  of uniformly doped surfaces can likely be attributed to changes in surface passivation. Improved surface passivation of doped regions that are distant from the bordering  $pn$ -junction reduces  $J_{01}$ . Due to the test structure design with constant area of  $p^+$  and  $n^+$  Si, such reduction in  $J_{01}$  is independent of the  $pn$ -junction density. On the other hand, improved passivation of the surface where the  $pn$ -junction borders will result in lower  $J_{02}$  values per density of  $pn$ -junctions. Notably, in some cases also an increase in  $J_{01}$  per junction density has been observed [e.g., Fig. 6(a)]. This indicates that the presence of a  $pn$ -junction can locally compromise the level of surface passivation. Presumably, the structuring process of the interdigitated  $pn$ -junction (such as the use of an diffusion mask) causes the formation of a residual doped glass layer in proximity of the junction that is harder to remove or changes in doping profiles near the  $pn$ -junction. This would result in a localized region where the surface passivation is negatively affected.

Besides surface recombination, potentially also an increased defect density in the c-Si bulk could be responsible for changes in  $pn$ -junction recombination for the different diffusion recipes, as bulk defects can also induce additional depletion region recombination and tunneling recombination at the  $pn$ -junction. To investigate this possibility, the influence of the diffusion recipes on the c-Si bulk material quality has been monitored. After carrying out the diffusion of boron and phosphorus, the highly doped regions were removed through wet-chemical etching, after which the c-Si surfaces were passivated by a-Si:H. For all three diffusion recipes, minority carrier lifetimes above 2 ms

TABLE I

SOLAR CELL PARAMETERS FOR MERCURY IBC CELLS WHICH WERE FABRICATED BY DIFFUSION RECIPES A AND C. THE REAR SURFACE WAS PASSIVATED BY A STACK OF  $\text{Al}_2\text{O}_3/\text{SiN}_x$ . THE RESULTS WERE OBTAINED FROM  $J$ - $V$  MEASUREMENTS UNDER STANDARD TEST CONDITIONS (25 °C, 1000 W/m<sup>2</sup>, AM1.5G) AND SUNS- $V_{oc}$  MEASUREMENTS ( $pFF$ ,  $J_{01}$ ,  $J_{02}$ ) AND REPRESENT THE AVERAGE OF SEVEN SOLAR CELLS. THE AREA OF EACH SOLAR CELL WAS 239 cm<sup>2</sup>.

	$J_{sc}$ (mA/cm <sup>2</sup> )	$V_{oc}$ (mV)	$FF$ (%)	$pFF$ (%)	$J_{01}$ (fA/cm <sup>2</sup> )	$J_{02}$ (nA/cm <sup>2</sup> )	$R_{Shunt}$ ( $\Omega$ )	$\eta$ (%)
Recipe A	39.6	627	73.8	79.2	733	46	9.4	18.3
Recipe C	40.1	643	75.0	80.7	421	24	8.9	19.3
Relative change (%)	1.2	2.7	1.6	1.9	-43	-48	-5.3	5.5

were measured, without a significant difference between the recipes. Therefore, it can be concluded that an increased level of bulk defects is an unlikely cause for the observed differences in  $pn$ -junction recombination between the three investigated diffusion recipes.

Finally, changing doping profiles can also affect the presence of a tunneling recombination current between  $p^+$  and  $n^+$  Si. In the literature, simulations on IBC cells show that for boron-doped regions with higher doping concentrations, the tunneling recombination increases and the shunt resistance reduces [18]. In this work, the various diffusion recipes result in minimal changes in the doping profiles (see Fig. 3), and a reduction in shunt resistance has not been observed (i.e., see Table I), making a significant change in tunnel recombination unlikely.

Therefore, on the basis of the discussion, the observed changes in  $pn$ -junction recombination for different diffusion recipes can most likely be attributed to differences in surface passivation quality. Nonetheless, more research would be required to corroborate this hypothesis.

## V. CONCLUSION

In this work, a method was presented to quantify charge-carrier recombination induced by the  $pn$ -junctions at the rear surface for IBC solar cells. The results underline that passivation of the c-Si surface (where  $pn$ -junctions border) is vital to reduce  $J_{02}$  recombination, which is in accordance with previous reports in the literature. Moreover, on the basis of this work, it can be concluded that, even after passivation of this surface, recombination at  $pn$ -junction can still be significant for IBC solar cells, resulting in  $V_{oc}$  losses of up to 10 mV. Therefore, it can be concluded that increasing the junction density—by e.g., reducing the pitch—will not necessarily improve the performance of IBC solar cells.

Besides surface passivation, the diffusion recipe for boron and phosphorus also had a strong impact on the presence of recombination at the  $pn$ -junction. In fact, by proper tuning of the diffusion processes, losses due to  $pn$ -junction recombination could be virtually eliminated, even in case of a *gapless*  $pn$ -junction. As a result of the improved diffusion recipe, the efficiency of industrially relevant “Mercury” IBC solar cells could be improved by 1% absolute.

The methods described in this work could be used for the evaluation of  $pn$ -junction recombination in other types of IBC solar cells as well, such as IBC cells which are based on doped a-Si:H or poly-Si carrier-selective contacts. Moreover, the results presented in this work are also relevant for other solar cell

architectures which can suffer from  $pn$ -junction recombination, such as multicrystalline or small area (cleaved) c-Si solar cells, where, respectively, the grain-boundaries or the cell perimeter are crossing the  $pn$ -junction.

## ACKNOWLEDGMENT

The authors would like to thank Dr. J. Melskens and Dr. L. E. Black from the Eindhoven University of Technology and Prof. A. W. Weeber, Dr. A. A. Mewe, Dr. L. J. Geerligs, and Dr. G. J. M. Janssen from ECN for their valuable contributions to this work.

## REFERENCES

- [1] C. Reichel, F. Granek, M. Hermle, and S. W. Glunz, “Investigation of electrical shading effects in back-contacted back-junction silicon solar cells using the two-dimensional charge collection probability and the reciprocity theorem,” *J. Appl. Phys.*, vol. 109, no. 2, 2011, Art. no. 24507.
- [2] I. Cesar, N. Guillemin, A. R. Burgers, and E. E. Bende, “MERCURY: A novel design for a back junction back contact cell with front floating emitter for high efficiency and simplified processing,” in *Proc. 29th Eur. Photovolt. Sol. Energy Conf. Exhib.*, 2014, pp. 681–688.
- [3] R. Müller *et al.*, “Analysis of  $n$ -type IBC solar cells with diffused boron emitter locally blocked by implanted phosphorus,” *Sol. Energy Mater. Sol. Cells*, vol. 142, pp. 54–59, Nov. 2015.
- [4] A. Mewe *et al.*, “Mercury: Industrial IBC cell with front floating emitter for 20.9% and higher efficiency,” in *Proc. 2015 IEEE 42nd Photovolt. Spec. Conf.*, vol. 9, 2015, pp. 1–6.
- [5] P. Spinelli *et al.*, “High resolution sheet resistance mapping to unveil edge effects in industrial IBC solar cells,” *Energy Procedia*, vol. 92, pp. 218–224, 2016.
- [6] D. J. Fitzgerald and A. S. Grove, “Surface recombination in semiconductors,” *IEEE Trans. Electron Devices*, vol. ED-15, no. 6, pp. 426–427, Jun. 1968.
- [7] A. S. Grove and D. J. Fitzgerald, “Surface effects on  $pn$  junctions: Characteristics of surface space-charge regions under non-equilibrium conditions,” *Solid State Electron.*, vol. 9, no. 8, pp. 783–806, 1966.
- [8] W. Shockley and W. T. J. Read, “Statistics of the recombinations of holes and electrons,” *Phys. Rev.*, vol. 87, no. 5, pp. 835–842, 1952.
- [9] R. N. Hall, “Electron-hole recombination in germanium,” *Phys. Rev.*, vol. 87, 1952, Art. no. 387.
- [10] C. T. Sah, R. N. Noyce, and W. Shockley, “Carrier generation and recombination in  $p$ - $n$  junctions and  $p$ - $n$  junction characteristics,” *Proc. IRE*, vol. 45, no. 9, pp. 1228–1243, 1957.
- [11] K. McIntosh, P. Altermatt, and G. Heiser, “Depletion-region recombination in silicon solar cells: When does  $mDR = 2$ ?” in *Proc. 16th Eur. Photovolt. Sol. Energy Conf.*, 2000, pp. 251–254.
- [12] C. H. Henry, R. A. Logan, and F. R. Merritt, “The effect of surface recombination on current in  $\text{Al}_x\text{Ga}_{1-x}\text{As}$  heterojunctions,” *J. Appl. Phys.*, vol. 49, no. 6, pp. 3530–3542, 1978.
- [13] G. A. M. Hurkx, D. B. M. Klaassen, and M. P. G. Knuvers, “A new recombination model for device simulation including tunneling,” *IEEE Trans. Electron Devices*, vol. 39, no. 2, pp. 331–338, Feb. 1992.
- [14] A. Schönecker *et al.*, “Attacking limiting factors in  $10 \times 10$  cm<sup>2</sup> multicrystalline silicon, emitter wrap-through solar cell design and processing,” in *Proc. 2nd World Conf. Photovolt. Sol. Energy Convers.*, Vienna, Austria, 1998, pp. 1677–1680.



- [15] R. Kuhn *et al.*, “11% semitransparent bifacially active power crystalline silicon solar cells,” in *Proc. 2nd world Conf. Exhib. Photovolt. Sol. Energy Convers.*, Vienna, Austria, 1998, pp. 1415–1417.
- [16] P. P. Altermatt, A. G. Aberle, J. Zhao, A. Wang, and G. Heiser, “A numerical model of  $p$ - $n$  junctions bordering on surfaces,” *Sol. Energy Mater. Sol. Cells*, vol. 74, nos. 1–4, pp. 165–174, Oct. 2002.
- [17] K. R. McIntosh, “Lumps, humps and bumps: Three detrimental effects in the current-voltage curve of silicon solar cells,” Ph.D. dissertation, Univ. New South Wales, Sydney N.S.W., Australia, 2001.
- [18] J. Dong *et al.*, “High-efficiency full back contacted cells using industrial processes,” *IEEE J. Photovolt.*, vol. 4, no. 1, pp. 130–133, Jan. 2014.
- [19] R. Peibst *et al.*, “High-efficiency RISE-IBC solar cells: Influence of rear side-passivation on  $pn$ -junction meander recombination,” in *Proc. 28th Eur. Photovolt. Sol. Energy Conf.*, 2013, pp. 971–975.
- [20] R. B. A. Merkle and R. Peibst, “High efficient fully ion-implanted, co-annealed and laser-structured back junction back contacted solar cells,” in *Proc. 29th Eur. Photovolt. Sol. Energy Conf. Exhib.*, 2014, pp. 954–958.
- [21] U. Römer *et al.*, “Ion implantation for poly-si passivated back-junction back-contacted solar cells,” *IEEE J. Photovolt.*, vol. 5, no. 2, pp. 507–514, Mar. 2015.
- [22] M. Rienäcker *et al.*, “Recombination behavior of photolithography-free back junction back contact solar cells with carrier-selective polysilicon on oxide junctions for both polarities,” *Energy Procedia*, vol. 92, pp. 412–418, 2016.
- [23] V. D. Mihailitchi, Y. Komatsu, and L. J. Geerligs, “Nitric acid pretreatment for the passivation of boron emitters for  $n$ -type base silicon solar cells,” *Appl. Phys. Lett.*, vol. 92, no. 6, 2008, Art. no. 63510.
- [24] A. Khanna *et al.*, “A fill factor loss analysis method for silicon wafer solar cells,” *IEEE J. Photovolt.*, vol. 3, no. 4, pp. 1170–1177, Oct. 2013.
- [25] N. Guillevin *et al.*, “Mercury: Industrial IBC Cell with front floating emitter for 20.9% and higher efficiency,” in *Proc. 2015 IEEE 42nd Photovolt. Spec. Conf.*, 2015, pp. 1–6.
- [26] M. Zanuccoli, P. Magnone, E. Sangiorgi, and C. Fiegna, “Analysis of the impact of geometrical and technological parameters on recombination losses in interdigitated back-contact solar cells,” *Sol. Energy*, vol. 116, pp. 37–44, 2015.
- [27] K. Rühle, M. K. Juhl, M. D. Abbott, L. M. Reindl, and M. Kasemann, “Impact of edge recombination in small-area solar cells with emitter windows,” *IEEE J. Photovolt.*, vol. 5, no. 4, pp. 1067–1073, Jul. 2015.
- [28] A. Richter, J. Benick, A. Kimmerle, M. Hermle, and S. W. Glunz, “Passivation of phosphorus diffused silicon surfaces with  $Al_2O_3$ : Influence of surface doping concentration and thermal activation treatments,” *J. Appl. Phys.*, vol. 116, no. 24, Dec. 2014, Art. no. 243501.
- [29] B. W. H. van de Loo *et al.*, “‘Zero-charge’  $SiO_2/Al_2O_3$  stacks for the simultaneous passivation of  $n^+$  and  $p^+$  doped silicon surfaces by atomic layer deposition,” *Sol. Energy Mater. Sol. Cells*, vol. 143, pp. 450–456, Dec. 2015.
- [30] D. E. Kane and R. M. Swanson, “Measurement of the emitter saturation current by a contactless photoconductivity decay method,” in *Proc. IEEE Photovolt. Spec. Conf.*, vol. 69, 1985, pp. 578–583.



**Bas W. H. van de Loo** was born in 's-Hertogenbosch, The Netherlands, in 1988. He received the M.Sc. and Ph.D. degrees in applied physics from the Eindhoven University of Technology (TU/e), Eindhoven, The Netherlands, in 2012 and 2017, respectively.

He is currently working as a Postdoctoral Researcher in the Plasma & Materials Processing Group of Prof. Erwin Kessels at the TU/e. In addition, he is a Process Development Engineer with Tempres Systems BV, Vaassen, The Netherlands.

From 2010 to 2011, he was an instructor of physics with the Fontys University of Applied Sciences, Eindhoven, The Netherlands. In 2011, he did a research internship in the group of Prof. Colin Wolden, Colorado School of Mines, Golden, CO, USA. His research interests include atomic layer deposition, boron diffusion, surface passivation, and transparent conductive oxides for silicon solar cells.



**Ard H. G. Vlooswijk** was born in Utrecht, The Netherlands, in 1979. He received the M.Eng. degree in solar energy engineering from Dalarna University, Falun, Sweden, in 2004, the M.Sc. degree in applied physics from the University of Twente, Enschede, The Netherlands, in 2005, and the Ph.D. degree in solid state chemistry from the University of Groningen, Groningen, The Netherlands, in 2009.

In 2003, he performed his internship at the Museum of Science & Technology for the exhibition “Nedkalla Solkraften” (Call down solar energy). From 2009 until 2016, he was a Process Development Engineer in the R&D Department, Tempres Systems BV, Vaassen. Currently, he is the Lead Metrology Engineer with Veco BV, Eerbeek, The Netherlands. He is the author of a book chapter on boron diffusion and of 13 peer-reviewed articles on ferroelectrics, diffusion, and photovoltaics. His main research interest focuses on thin film deposition of functional layers and their (electrical) characterization. It also includes their application as electrodes, ferroelectric, and photovoltaic devices.

Dr. Vlooswijk was actively involved in the cooperation receiving the High-Tech Systems Platform Action Award 2012 and the WNF Cleantech Star 2012.



**W. M. M. (Erwin) Kessels** received the M.Sc. and Ph.D. degrees (*cum laude*) in applied physics from the Eindhoven University of Technology (TU/e), Eindhoven, The Netherlands, in 1996 and 2000, respectively.

He is a Full Professor with TU/e, where he is also the Scientific Director of the NanoLab@TU/e clean room facilities. His research interests include the field of synthesis of ultrathin films and nanostructures using methods such as (plasma-enhanced) chemical vapor deposition and atomic layer deposition

(ALD) for a wide variety of applications. As such, he has pioneered the application of ALD and  $Al_2O_3$  films for the surface passivation of crystalline silicon solar cells, and currently, he is exploring the use of ALD in many more types of solar cells.



**Ilkay Cesar** was born in Wuppertal-Barmen, Germany, in 1975. He received the Master's degree in chemical engineering from the Delft University of Technology, Delft, The Netherlands, in 2001, and the Ph.D. degree in chemistry and chemical engineering from the École Polytechnique Fédérale de Lausanne, Lausanne, Switzerland, in 2007.

Since 1998, he has been involved in the field of solar energy conversion into electricity or fuels. He researched devices ranging from dye-sensitized solar cells to photoelectrochemical tandem cells based on nanostructured ironoxide ( $\alpha$ -hematite) for the purpose of solar-driven water-splitting. In 2007, he joined ECN Solar Energy, Petten, The Netherlands, and is currently focusing on the industrialization of new silicon PV technology. In the capacity of a Senior Researcher, he is leading international projects in tight partnership with Dutch industry. The recent implementation of bifacial IBC solar cell technology at Yingli Solar is a good example of this work.

Dr. Cesar received the “Du Pont Material award” for excellent research in the field of material science related to solar fuels for his Ph.D. dissertation.



**Pierpaolo Spinelli** was born in Putignano, Italy, in 1985. He received the Master's (*cum laude*) degree in physics from the University of Padova, Padova, Italy, and the Graduate (*cum laude*) degree in Natural Sciences from the Galileian School of Higher Education, Padova Italy, both in 2009, and the Ph.D. degree in physics from the University of Amsterdam, Amsterdam, The Netherlands, in 2013, with a thesis on light trapping in silicon solar cells using resonant nanostructures. The Ph.D. work was performed at the FOM Institute for Atomic and Molecular Physics, Amsterdam, The Netherlands.

Since 2014, he has been working as a Research Scientist with the Energy Center of the Netherlands, Petten, The Netherlands. He is the author of 14 peer-reviewed articles in the field of solar energy, with more than 900 citations. His work is currently focused on bifacial IBC solar cells and novel concepts for PV, such as light trapping nanostructures and novel materials for passivated contacts.